The ISSP International Workshop, “New Horizon of Strongly Correlated Physics” (NHSCP2014)

Dynamics change at the Mott transition: examination of doublon dynamics in a triangular-lattice Hubbard model

Toshihiro Sato

(Computational Condensed Matter Physics Laboratory, RIKEN)

Hirokazu Tsunetsugu

(Institute for Solid State Physics, University of Tokyo)

Acknowledge; Kazumasa Hattori

(Institute for Solid State Physics, University of Tokyo)

Outline

- Introduction : Mott metal-insulator transition
- Model and method:
- Numerical results:
  Nearest-neighbor (on-site) dynamical correlations of doublon
- Summary

Outline

- Introduction : Mott metal-insulator transition
- Model and method:
- Numerical results:
  Nearest-neighbor (on-site) dynamical correlations of doublon
- Summary

Mott metal-insulator transition

- Mott insulator N. F. Mott, Proc. R. Soc. London, Ser. 1949
  - ・Strong Coulomb repulsion
  - ・Electron density of the system n=1
  - ・Spin internal degrees of freedom→ magnetic transition

- Theoretical understanding of the Mott transition has been studied in the Hubbard model by using several numerical methods, DMFT (CDMFT), VCA, VMC,……

$$H = \sum_{i,j,\sigma} v_{ij} c^{\dagger}_{i\sigma} c_{j\sigma} - \mu \sum_{i,\sigma} c^{\dagger}_{i\sigma} c_{i\sigma} + U \sum_{i} n_{i\uparrow} n_{i\downarrow}$$

$v_{ij} = v$; nearest neighbor hopping amplitude
U ; Coulomb repulsion
μ ; chemical potential
$c^{\dagger}_{i\sigma}$ ($c_{i\sigma}$) ; electron creation (annihilation) operator at site i with spin σ
$n_{i\sigma} = c^{\dagger}_{i\sigma} c_{i\sigma}$; electron density operator

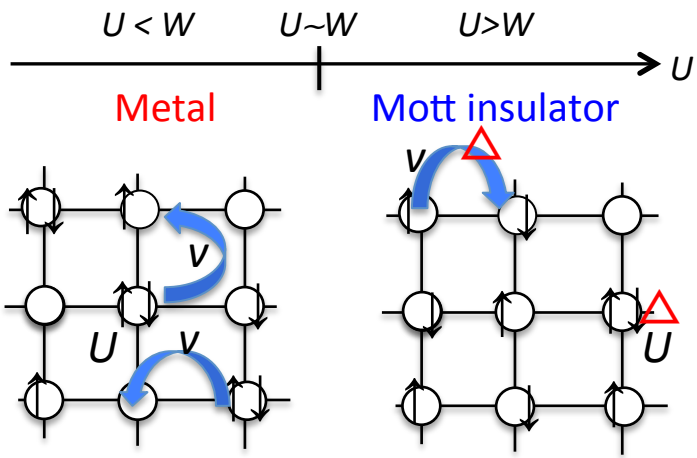

↑(↓) : electron with spin up (down)

- Mott transition in the single-band Hubbard model for fixed electron density n=1

∗ Coulomb repulsion U ⇔ electronic kinetic energy W
(it is not accompanied by magnetic transition)

Mott metal-insulator transition

- Relevant variables in the Mott transition:

  C. Castellani et al., PRL 1979

  Doublon (doubly occupied site) density

$$d = \langle n_{i\uparrow} n_{i\downarrow} \rangle$$

  $n_{i\sigma}$; electron density operator at site i with spin σ

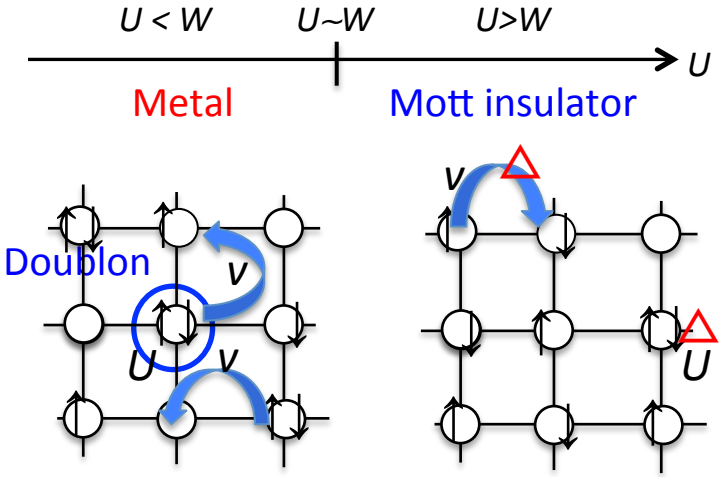

  * For U>>W, the Hubbard model becomes equivalent to the Heisenberg model.

  ☞The relevant variables are the local spin operators, each site being occupied by one electron with either spin up or spin down.

  ☞However, when U>>W does not hold, such a description is no longer valid and doublons and holon (vacant sites) will also occur.

- Determination of finite-temperature phase diagram in the DMFT (CDMFT) calculations

  ・Infinite dimension

  A. Georges et al., Rev Mod Phys. 2011

  ・Frustration lattice ; triangular lattice, kagome lattice……

  R. Zitzler et al., PRL 2004 B. Kyung et al., PRL 2006

  T. Ohashi et al., PRL 2006/PRL 2008 A. Liebsch et al., PRB 2009

  Y. Furukawa et al., PRB 2010

Finite-temperature phase diagram in the DMFT calculations

✧ Infinite dimension (DMFT)

A. Georges et al., Rev Mod Phys. 2011

- Paramagnetic solution
- half-filling

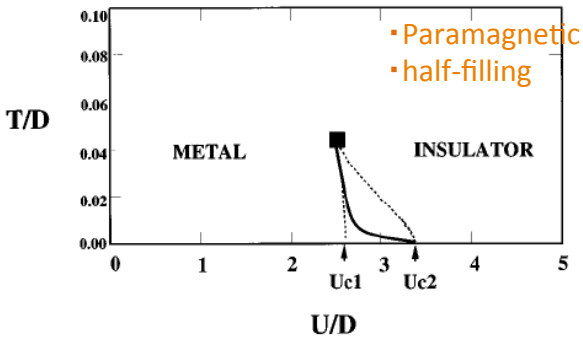

FIG. 33. Phase diagram of the fully frustrated model at half-filling. It is possible to move continuously from one phase to the other since at high temperature the transition becomes a crossover. Within the region delimited by the dashed lines, the metallic and insulating solutions coexist. The full line is the approximate location of the actual first-order transition line. Both ends of this line [at the full square and at $U_{c2}(T)=0$] are second-order points.

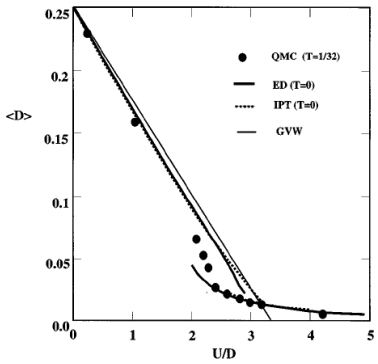

FIG. 34. Double occupancy $\langle D\rangle=\langle n_\uparrow n_\downarrow\rangle$ as a function of the interaction U/D. The data corresponds to QMC simulations at $\beta D=32$ (dots), eight sites exact diagonalization (bold line) and iterated perturbation theory at $T=0$ (dotted line). For comparison, the results of the Gutzwiller approximation is also plotted (thin line).

✧ Anisotropic triangular lattice (CDMFT)

T. Ohashi et al., PRL 2008

- Paramagnetic solution
- half-filling

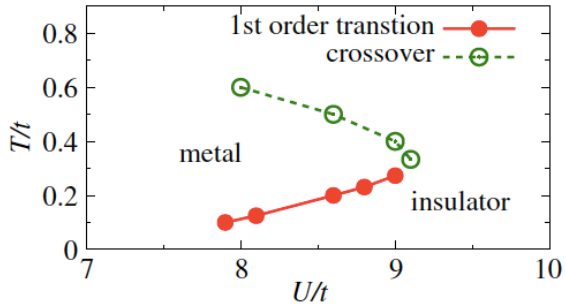

FIG. 1 (color online). Phase diagram of Hubbard model on anisotropic triangular lattice for $t'/t = 0.8$.

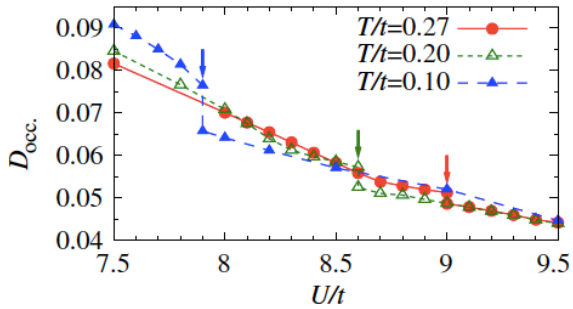

FIG. 4 (color online). Double occupancy as a function of interaction strength U/t for $t'/t = 0.8$ at several temperatures. We show only the transition from insulator to metal with weakening U (defined as U_{c1}), although we find hysteresis.

Thermodynamic criticality of the Mott transition

- Investigation of the singularity of doublon density near the Mott critical end point

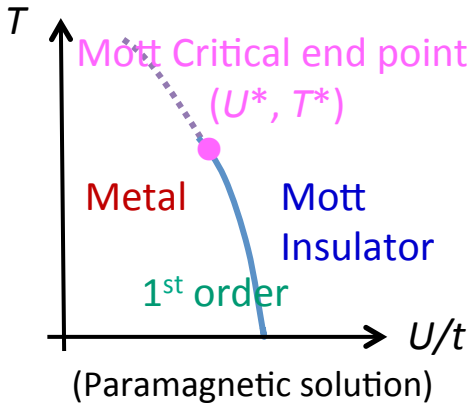

(Paramagnetic solution)

$$d - d^* = \left|U - U^*\right|^{1/\delta}; T = T^*$$

G. Kotliar et al., PRL 2000
M. Imada, PRB 2005
P. Sémon et al., PRB 2012

Ising		Mott
m	⇔	d–d*
h		U–U*
T		T

✧ Ising universality class (UC)

- Anisotropic triangular lattice Hubbard model (paramagnetic solution)

P. Sémon et al., PRB 2012

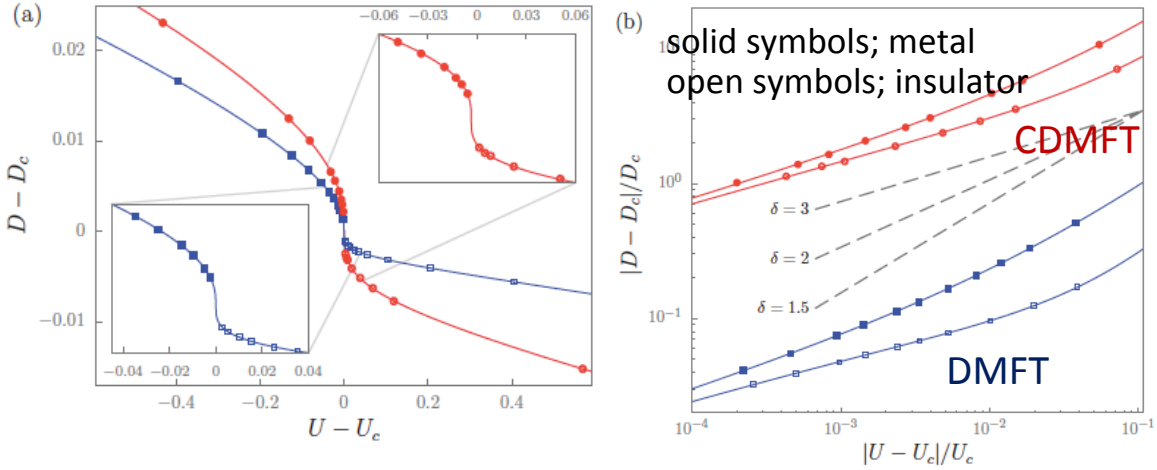

FIG. 3. (Color online) Double occupancy as a function of U near the Mott critical point for the Hubbard model on an anisotropic triangular lattice with $t'/t = 0.8$ ($t \equiv 1$) at half filling and fixed critical inverse temperature $\beta = 11.15$ (squares) for DMFT and $\beta = 9.9$ (circles, shiftet by $\times 10^{1.5}$) for CDMFT on a 2×2 plaquette. The solid lines show a fit to $f(U) = c_1 \mathrm{sgn}(\delta U)|\delta U|^{1/\delta} + c_2|\delta U|^{2/\delta} + c_3 \delta U + D_c$ ($\delta U \equiv U - U_c$) with the same parameters c_1, c_2, c_3, D_c, U_c, and δ for the metallic (filled symbols) and the insulating region (open symbols). The best fitting values (U_c, D_c, δ) are (10.445,0.0325,2.93) for DMFT and (7.932,0.0679,3.04) for CDMFT. (a) Linear plot centered at (U_c, D_c). The insets zoom on the regions close to the critical point. (b) Logarithmic plot in reduced units relative to the critical point with CDMFT data shifted by a factor of $10^{1.5}$ along the y axis. The dashed lines show the function $\propto |U - U_c|^{1/\delta}$ with δ as indicated. In the critical regime, up to 500 iterations are necessary for convergence in the iterative solution of the (C)DMFT equation. Once convergence is reached, we take the average over hundreds of iterations. Monte Carlo sweeps per iteration: 6×10^9 for DMFT and 10^9 for CDMFT.

Mechanism of Mott metal-insulator transition

- Correlations between doublon (double occupied site) and holon (vacant site) and between two doublons have been studied in the square-lattice Hubbard model at half-filling without magnetic order by VMC method.

  T. Miyagawa and H. Yokoyama, JPSJ 2011

∗ Assumption: Attraction between doublon and holon
Repulsion between two doublons

∗ They investigated the variation of two correlations with *U*.

$l_{DH} = \langle r_{DH} \rangle + \sigma_{DH}$

:maximum distance between doublon and holon (doublon-holon binding length)

$l_{DD} = \langle r_{DD} \rangle + \sigma_{DD}$

:minimum distance between two doublons (doublon-doublon exclusion length)

$\langle r_{OO'} \rangle$; average nearest OO' distance

$\sigma_{OO'}$; standard deviation of $\langle r_{OO'} \rangle$

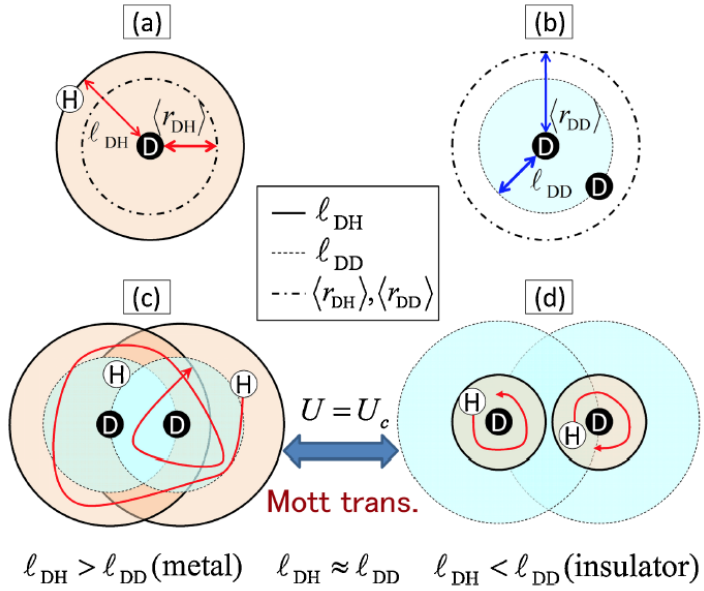

Fig. 15. (Color online) Schematic figures of microscopic mechanism of the Mott transition. (a) The solid circle of radius ℓ_{DH} denotes the domain in which a holon can itinerate, when the partner doublon is located at the center. (b) The solid circle of radius ℓ_{DD} denotes the forbidden area where a doublon cannot enter, when another doublon is situated at the center. In (c) and (d), the behaviors of doublons (D) and holons (H) are illustrated for the metallic and insulating states, respectively, in ordinary D–H binding wave functions. The explanation is given in §4.1. The two phases are distinguished by comparing the magnitude of ℓ_{DH} and ℓ_{DD}.

Mechanism of Mott metal-insulator transition

- Correlations between doublon (double occupied site) and holon (vacant site) and between two doublons have been studied in the square-lattice Hubbard model at half-filling without magnetic order by VMC method.

  T. Miyagawa and H. Yokoyama, JPSJ 2011

∗ Assumption: Attraction between doublon and holon
Repulsion between two doublons

∗ They investigated the variation of two correlations with *U*.

$l_{DH} = \langle r_{DH} \rangle + \sigma_{DH}$

:maximum distance between doublon and holon (doublon-holon binding length)

$l_{DD} = \langle r_{DD} \rangle + \sigma_{DD}$

:minimum distance between two doublons (doublon-doublon exclusion length)

$\langle r_{OO'} \rangle$; average nearest OO' distance

$\sigma_{OO'}$; standard deviation of $\langle r_{OO'} \rangle$

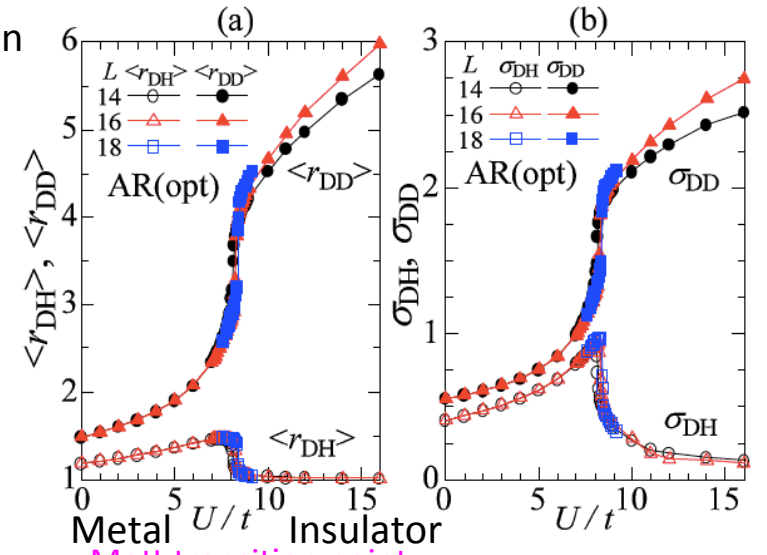

Fig. 14. (Color online) (a) The nearest D-to-H and H-to-D distances and nearest D-to-D and H-to-H distances calculated with AR(opt) are plotted for three system sizes as functions of the interaction strength. (b) Standard deviations of $\langle r_{DH} \rangle$ and $\langle r_{DD} \rangle$ shown in (a).

Mechanism of Mott metal-insulator transition

- Correlations between doublon (double occupied site) and holon (vacant site) and between two doublons have been studied in the square-lattice Hubbard model at half-filling without magnetic order by VMC method.

  T. Miyagawa and H. Yokoyama, JPSJ 2011

∗ Assumption: Attraction between doublon and holon
Repulsion between two doublons

∗ They investigated the variation of two correlations with U.

$l_{DH} = \langle r_{DH} \rangle + \sigma_{DH}$

:maximum distance between doublon and holon (doublon-holon binding length)

$l_{DD} = \langle r_{DD} \rangle + \sigma_{DD}$

:minimum distance between two doublons (doublon-doublon exclusion length)

$\langle r_{OO'} \rangle$; average nearest OO' distance

$\sigma_{OO'}$; standard deviation of $\langle r_{OO'} \rangle$

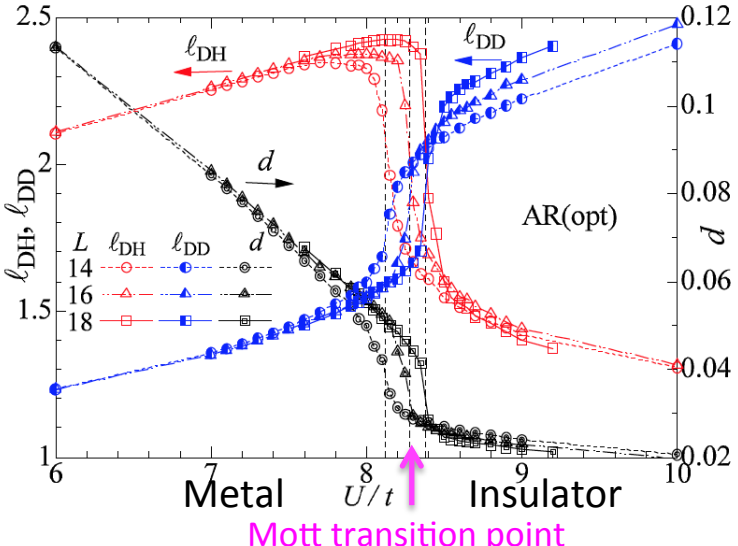

Fig. 16. (Color online) The D–H binding length ℓ_{DH} and the D–D exclusion distance ℓ_{DD} for AR(opt) obtained from the data in Fig. 14 are plotted as functions of U/t. For comparison, the doublon density and critical values obtained thereby (vertical dashed lines) are added for the same systems.

✧They suggested that the change of doublon–holon and doublon-doublon correlations is the essence of the Mott transition.

・At the Mott transition point, l_{DH} show drastically drop.

⇒Strong doublon-holon correlation in the insulating phase

Mechanism of Mott metal-insulator transition

- Correlations between doublon (double occupied site) and holon (vacant site) and between two doublons have been studied in the square-lattice Hubbard model at half-filling without magnetic order by VMC method.

  T. Miyagawa and H. Yokoyama, JPSJ 2011

∗ Assumption: Attraction between doublon and holon
Repulsion between two doublons

∗ They investigated the variation of two correlations with U.

$l_{DH} = \langle r_{DH} \rangle + \sigma_{DH}$

:maximum distance between doublon and holon (doublon-holon binding length)

$l_{DD} = \langle r_{DD} \rangle + \sigma_{DD}$

:minimum distance between two doublons (doublon-doublon exclusion length)

$\langle r_{OO'} \rangle$; average nearest OO' distance

$\sigma_{OO'}$; standard deviation of $\langle r_{OO'} \rangle$

✧ **Dynamics of doublons ??**

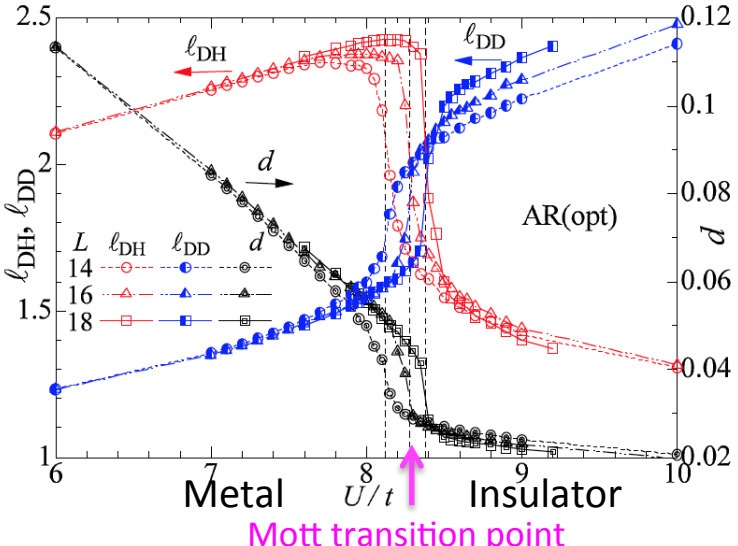

Fig. 16. (Color online) The D–H binding length ℓ_{DH} and the D–D exclusion distance ℓ_{DD} for AR(opt) obtained from the data in Fig. 14 are plotted as functions of U/t. For comparison, the doublon density and critical values obtained thereby (vertical dashed lines) are added for the same systems.

Outline

- Introduction : Mott metal-insulator transition
- **Model and method:**
- Numerical results:
  Nearest-neighbor (on-site) dynamical correlations of doublon
- Summary

Model and Method

- We study dynamics of doublons in the half-filed Hubbard Model.

$$H = \sum_{i,j,\sigma} v_{ij} c^{\dagger}_{i\sigma} c_{j\sigma} - \mu \sum_{i,\sigma} c^{\dagger}_{i\sigma} c_{i\sigma} + U \sum_{i} n_{i\uparrow} n_{i\downarrow}$$

v_{ij} =v; nearest neighbor hopping amplitude
U ; Coulomb repulsion
μ ; chemical potential

✓ Triangular lattice: Mott transition occurs inside the paramagnetic region.
VCA calculations : P. Sahebsara et al., PRL 2008, A. Yamada, PRB 2014

⇒ We can capture the dynamical properties of only Mott transition.

- Nearest-neighbor (on-site) dynamical correlations of doublon, holon, and single-occupied site

$$S^{j}_{oo'}(t) = \left\langle \hat{o}_1(t) \hat{o}'_j(0) \right\rangle$$

$j = 1$; on site
$j = 2 = 3$; nearest - neighbor sites

$\hat{o}_j = \hat{d}_j$; doublon density
$= \hat{h}_j$; holon density
$= \hat{s}_j$; single - occupied density

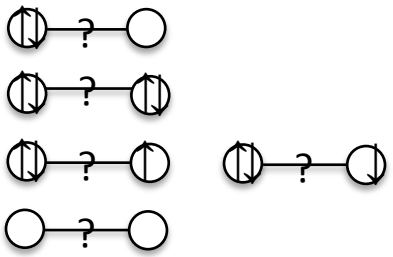

↑(↓) : electron with spin up (down)

✓ Cellular Dynamical Mean Field Theory (CDMFT)
G. Kotliar et al., PRL 2001

- Triangular 3-site cluster
- Numerical solver:
  Continuous-time Quantum Monte Carlo(CTQMC)
  Method based on strong coupling expansion
  P. Werner et al., PRL 2006
- Paramagnetic solution

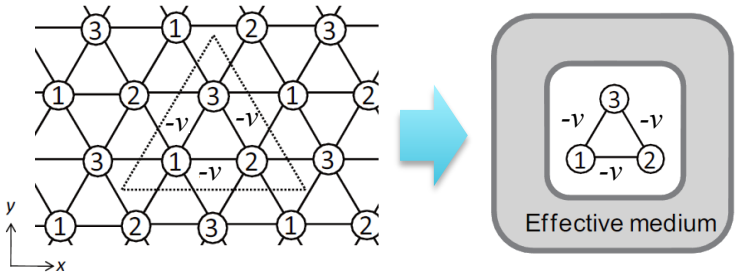

Outline

- Introduction : Mott metal-insulator transition
- Model and method:
- **Numerical results:**
  Nearest-neighbor (on-site) dynamical correlations of doublon
- Summary

Finite-*T* Mott transition: *U*-*T* phase diagram

- We investigate the singularity of the doubon density with changing *U* at several *T*'s

$d = \langle n_{i\uparrow} n_{i\downarrow} \rangle$ $n_{i\sigma}$; electron density operator at site i with spin σ

U-dependence of *d*

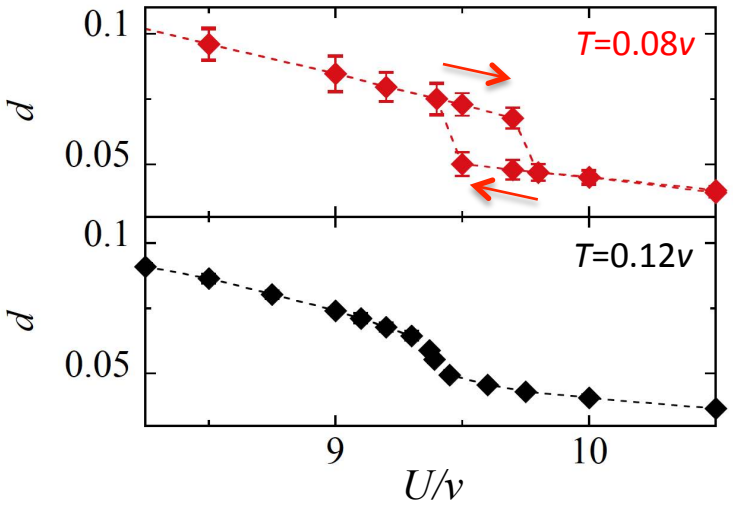

DOS

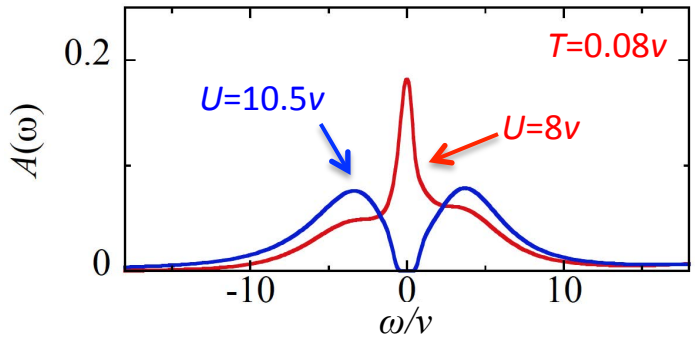

U-*T* phase diagram

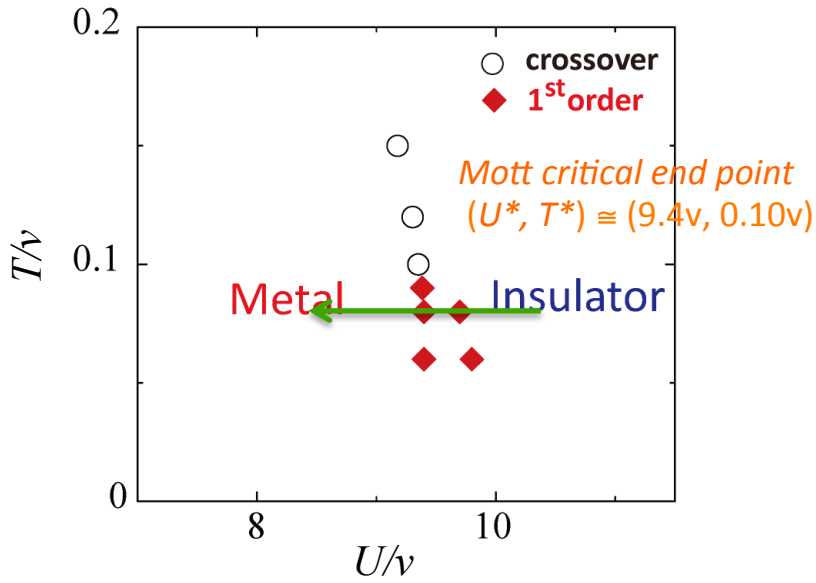

✧ We investigate doublon dynamics with decreasing *U* at *T*=0.08*v* <*T** fixed, where the first-order Mott transition occurs at U_c=9.4*v*.

Dynamical correlations between nearest-neighbor sites

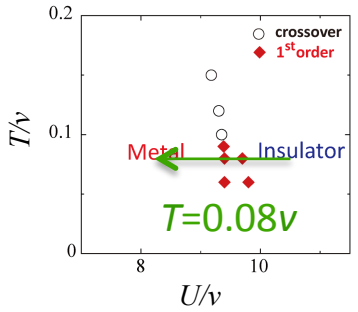

◘ Equal-time correlations, t=0 : $\langle \hat{o}_1 \hat{o}_2' \rangle$

$$P^{oo'} = \frac{\langle \hat{o}_1 \hat{o}_2' \rangle}{\langle \hat{o}_1 \rangle \langle \hat{o}_2' \rangle}$$

$\hat{o}_j = \hat{d}_j$; doublon density

$= \hat{h}_j$; holon density

$= \hat{s}_j$; single-occupied density

P^{dh} P^{dd} P^{ds} P^{hh}

∗ At U=0, $P^{oo'}$=1

∗ Equal-time correlation between nearest-neighbor sites

- $P^{oo'}$>1: attraction
- $P^{oo'}$<1: repulsion

U-dependence of $P^{oo'}$

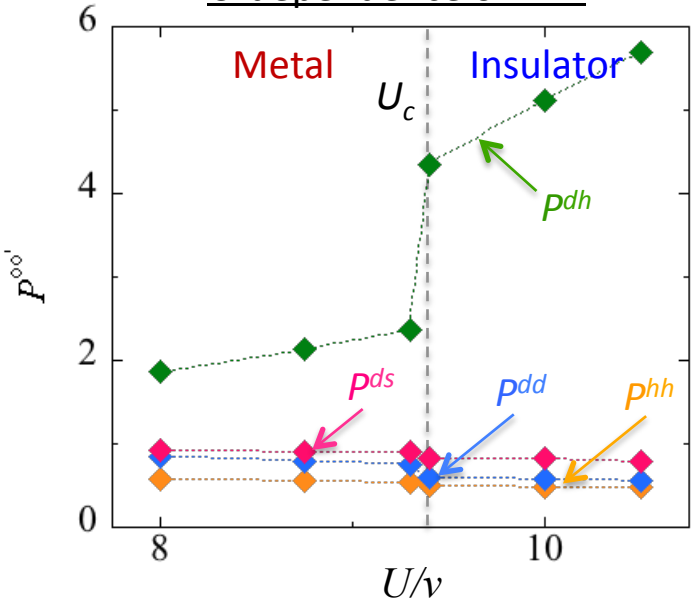

✧ P^{dh}>1 and takes a large value.
⇒Strong nearest-neighbor attraction
Enhancement at the Mott transition

✧ P^{dd}<1, P^{ds}<1, P^{hh}<1
⇒Nearest-neighbor repulsion
Their enhancement at the Mott transition is not as large as that of doublon holon attraction.

Dynamical correlations between nearest-neighbor sites

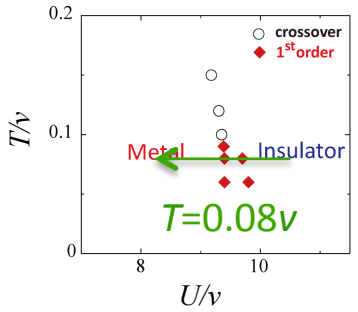

$$\Gamma^2_{oo'}(t) = \left|S^2_{oo'}(t)\right| - \left|\langle\hat{o}_1\rangle\langle\hat{o}'_2\rangle\right| \qquad S^2_{oo'}(t) = \langle\hat{o}_1(t)\hat{o}'_2(0)\rangle \xrightarrow{t\to\infty} \langle\hat{o}_1\rangle\langle\hat{o}'_2\rangle$$

- characteristic of the nearest-neighbor correlation:

$\Gamma^2_{oo'}(t) > 0$: attractive correlation $\Gamma^2_{oo'}(t) < 0$: repulsive correlation

doublon-holon

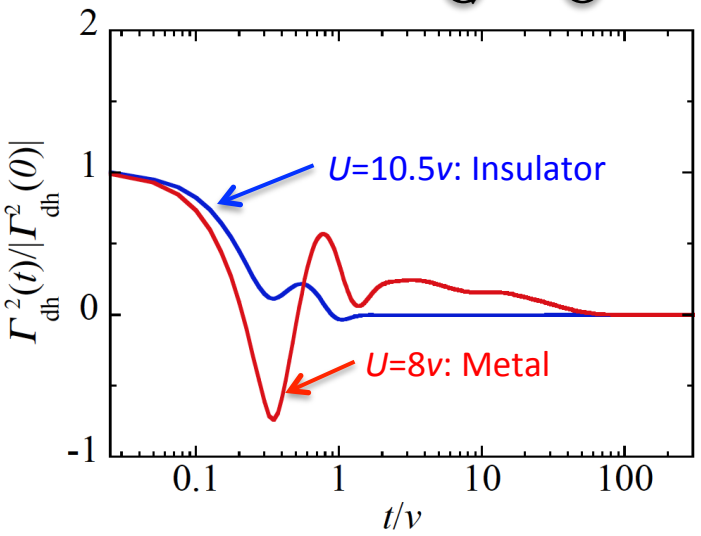

doublon-doublon

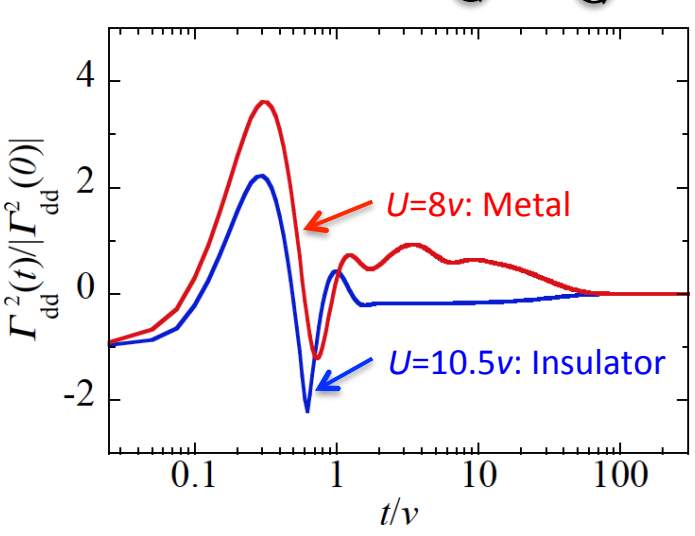

✧ Short-*t* behavior:

- The doublon-holon pair decays with increasing *t* and its lifetime becomes longer in the insulating phase.
- The doublons pair starts to be dynamically formed and its formation occurs faster in the metallic phase than in the insulating phase.

Dynamical correlations between nearest-neighbor sites

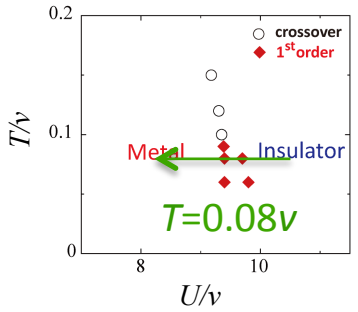

$$\Gamma^2_{oo'}(t) = \left|S^2_{oo'}(t)\right| - \left|\langle\hat{o}_1\rangle\langle\hat{o}'_2\rangle\right| \qquad S^2_{oo'}(t) = \langle\hat{o}_1(t)\hat{o}'_2(0)\rangle \xrightarrow{t\to\infty} \langle\hat{o}_1\rangle\langle\hat{o}'_2\rangle$$

- characteristic of the nearest-neighbor correlation:

$\Gamma^2_{oo'}(t) > 0$: attractive correlation $\Gamma^2_{oo'}(t) < 0$: repulsive correlation

doublon-holon

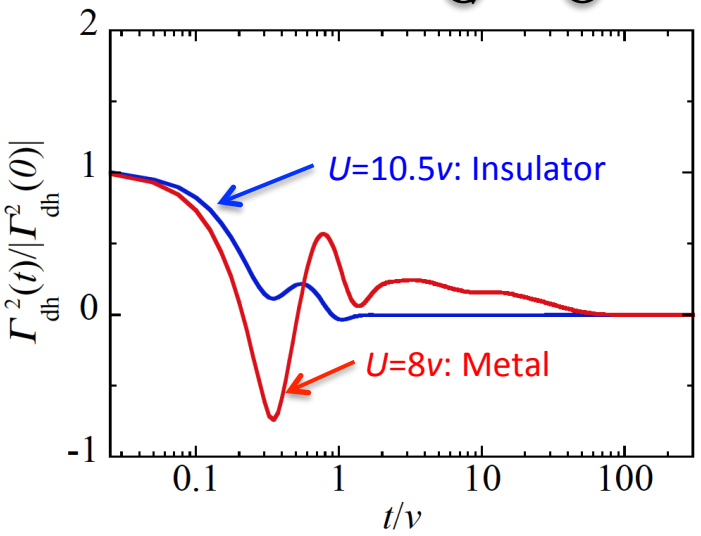

doublon-doublon

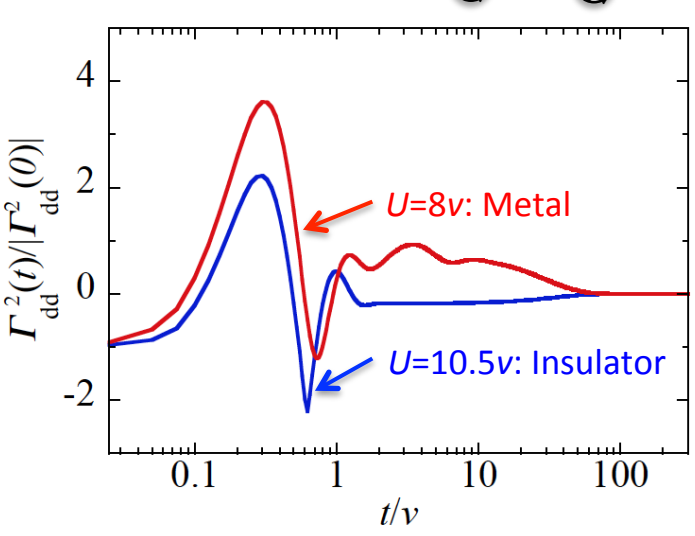

✧ Long-*t* behavior:

- In the insulating phase, $\Gamma_{oo'}{}^2$(t/v>2) is almost vanishing.
- In the metallic phase, $\Gamma_{oo'}{}^2$(t) persists up to long t/v~50.
- The t-dependence in the metallic phase shows many structures.

⇒larger charge fluctuation in the metallic phase

Dynamical correlations between nearest-neighbor sites

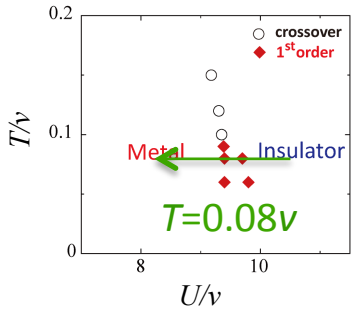

$$\Gamma^2_{oo'}(t) = \left|S^2_{oo'}(t)\right| - \left|\langle\hat{o}_1\rangle\langle\hat{o}'_2\rangle\right| \qquad S^2_{oo'}(t) = \langle\hat{o}_1(t)\hat{o}'_2(0)\rangle \xrightarrow{t\to\infty} \langle\hat{o}_1\rangle\langle\hat{o}'_2\rangle$$

- characteristic of the nearest-neighbor correlation:

$\Gamma^2_{oo'}(t) > 0$: attractive correlation $\Gamma^2_{oo'}(t) < 0$: repulsive correlation

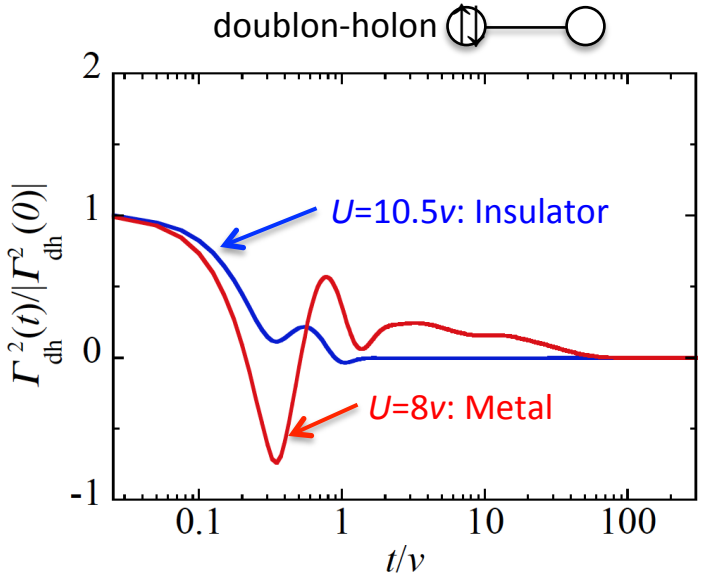

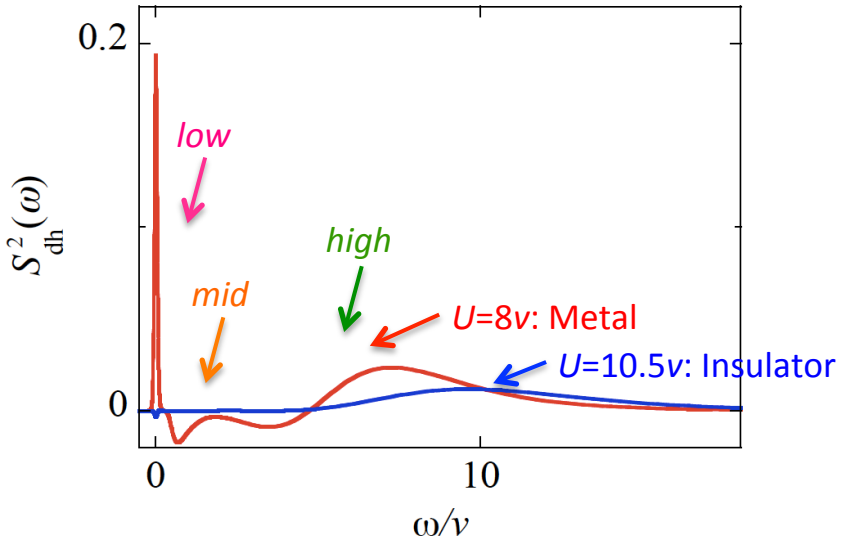

On-site dynamical correlation of doublon

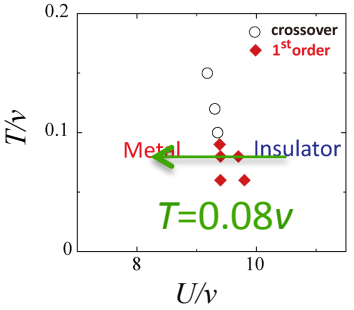

$$\Gamma^1_{dd}(t) = \left|S^1_{dd}(t)\right| - \left|\left\langle \hat{d}_1 \right\rangle \left\langle \hat{d}_1 \right\rangle\right|$$

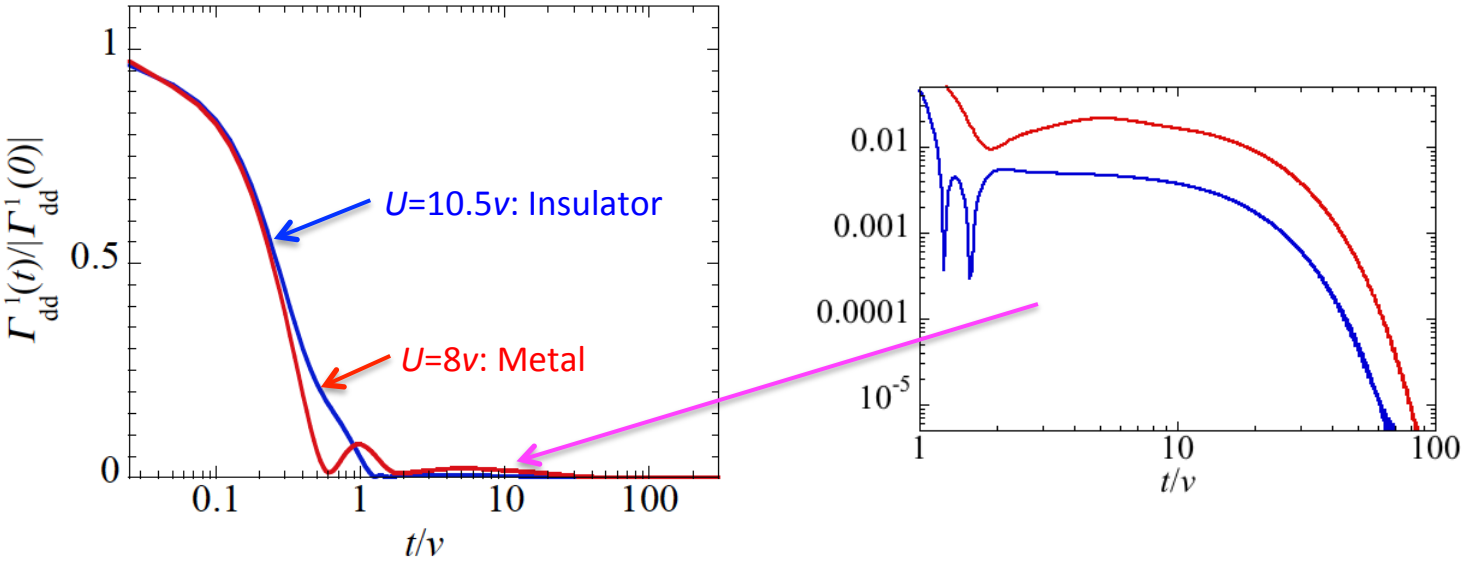

✧ $\Gamma_{dd}^1(t)$ decreases with t for both phases, but this decrease is not monotonic.
✧ This relaxation time towards 0 is related with the doublon lifetime.
⇒Its lifetime is longer in the metallic phase than in the insulating phase.

On-site dynamical correlation of doublon

$$\Gamma^1_{dd}(t) = \left|S^1_{dd}(t)\right| - \left|\left\langle \hat{d}_1 \right\rangle \left\langle \hat{d}_1 \right\rangle\right|$$

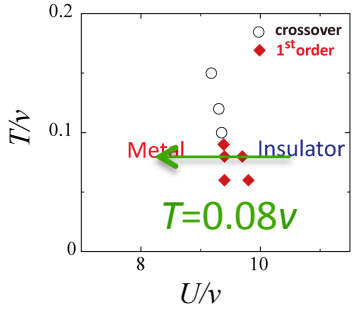

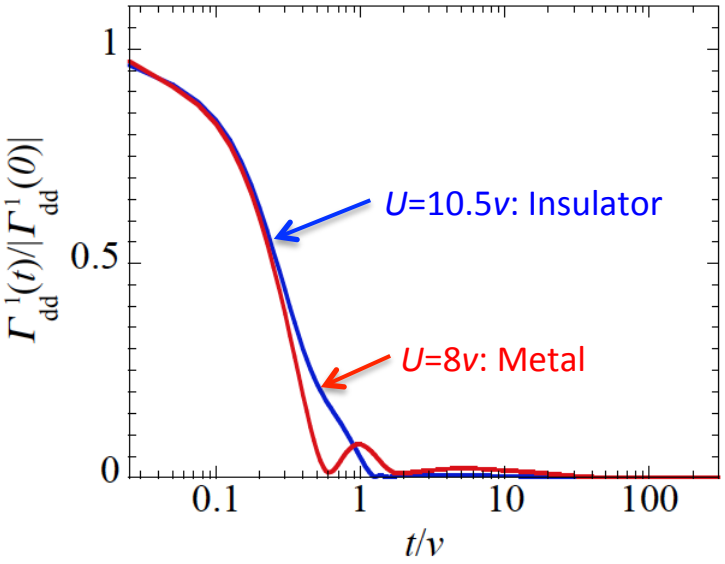

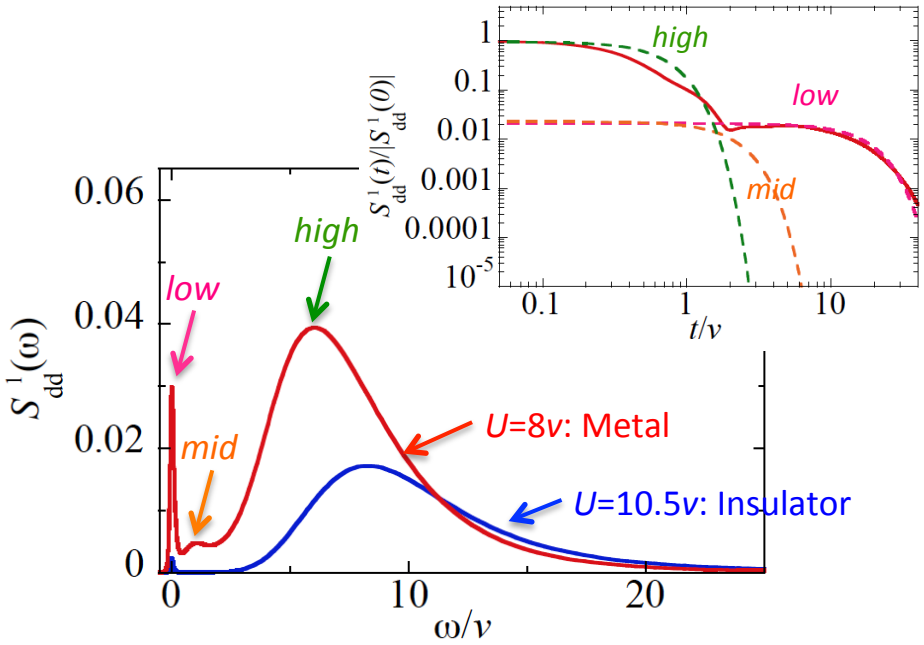

✧ Γ_{dd}^1(t) decreases with t for both phases, but this decrease is not monotonic.

✧ This relaxation time towards 0 is related with the doublon lifetime.

⇒Its lifetime is longer in the metallic phase than in the insulating phase.

✧ Two characteristic structures at t/v~0.6 and 2

- t/v~0.6: the contribution from middle-ω part of S_{dd}^1(ω) changes.
- t/v~2 : the change from the contribution of high-ω part to that of the low-ω part occurs.

Summary

- We have numerically studied doublon dynamics in the half-filled Hubbard Model on a triangular lattice by using the cellular dynamical mean field theory.
- We have demonstrated clear differences of dynamics of doublon between in the metallic and in the insulating phases.

✧ Nearest-neighbor dynamical correlations of doublon and holon :

- The nearest-neighbor doublon-holon pair shows a strong attraction, in particular in the insulating phase.
- The nearest-neighbor pairs between doublons, between holons, and between doublon and single occupied site show a repulsion.
- In short-time behaviors, the lifetime of doublon-holon pair becomes longer in the insulating phase and the formation of doubon pairs occurs faster in the metallic phase.
- In longer-time behaviors, their correlations persist up to more long time in the metallic phase.

✧ On-site dynamical correlation of doublon shows that doublons in the metallic phase have a longer lifetime than that in the insulating phase.

Toshihiro Sato and Hirokazu Tsunetsugu, arXiv:1404.6598

Mechanism of Mott metal-insulator transition

- Correlations between doublon (double occupied site) and holon (vacant site) and between two doublons have been studied in the square-lattice Hubbard model at half-filling without magnetic order by VMC method.

  T. Miyagawa and H. Yokoyama, JPSJ 2011

Table I. Summary of trial wave functions. In the second column, we abbreviate the type of correlation, with GW being the onsite (Gutzwiller) repulsion.

Ψ abbreviation	Correlation type	Correlation range	Parameter number
GWF	GW	Onsite	1
A(NN)	GW+DH	NN	2
A(bind)	GW+DH	NN	1
A(exp)	GW+DH	Long	2
R(exp)	GW+DD	Long	3
AR(exp)	GW+DH+DD	Long	4
A(pow)	GW+DH	Long	2
R(pow)	GW+DD	Long	3
AR(pow)	GW+DH+DD	Long	4
A(opt)	GW+DH	Long	L
R(opt)	GW+DD	Long	$L+1$
AR(opt)	GW+DH+DD	Long	$2L$

Dynamical correlations between nearest-neighbor sites

$$\Gamma^2_{oo'}(t) = \left|S^2_{oo'}(t)\right| - \left|\langle\hat{o}_1\rangle\langle\hat{o}'_2\rangle\right| \qquad S^2_{oo'}(t) = \langle\hat{o}_1(t)\hat{o}'_2(0)\rangle \xrightarrow{t\to\infty} \langle\hat{o}_1\rangle\langle\hat{o}'_2\rangle$$

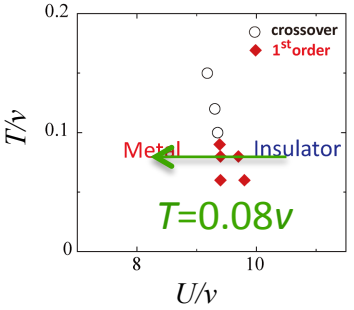

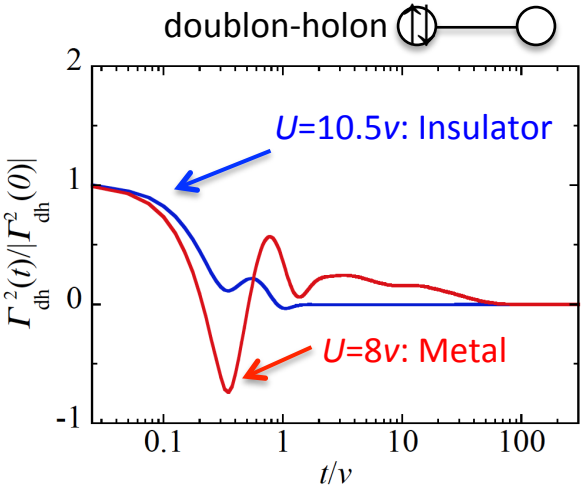

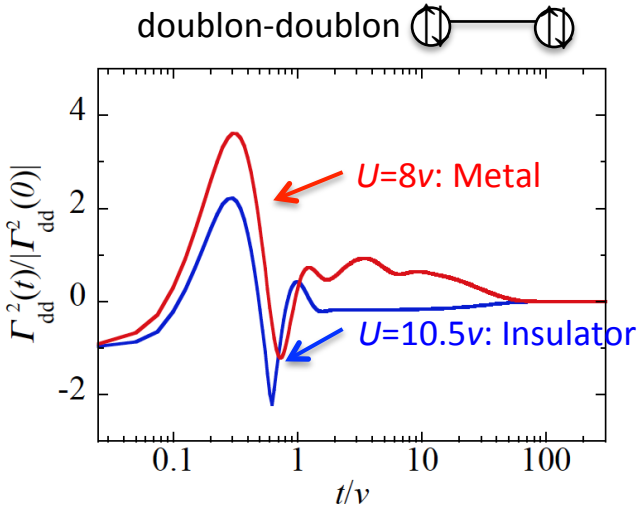

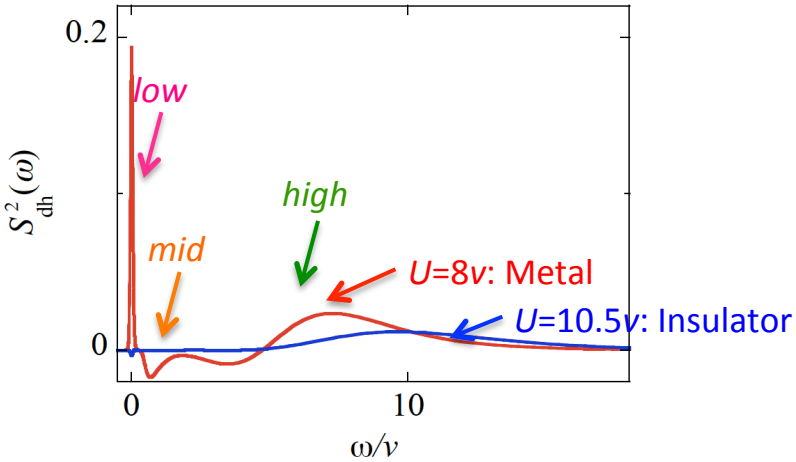

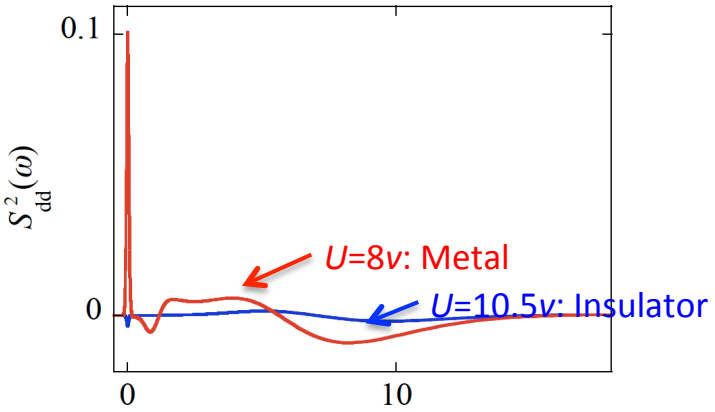

Dynamical correlations between nearest-neighbor sites

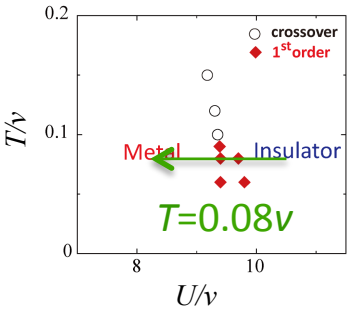

$$\Gamma^2_{oo'}(t) = \left|S^2_{oo'}(t)\right| - \left|\langle\hat{o}_1\rangle\langle\hat{o}'_2\rangle\right| \qquad S^2_{oo'}(t) = \langle\hat{o}_1(t)\hat{o}'_2(0)\rangle \xrightarrow{t\to\infty} \langle\hat{o}_1\rangle\langle\hat{o}'_2\rangle$$

- characteristic of the nearest-neighbor correlation:

$\Gamma^2_{oo'}(t) > 0$: attractive correlation

$\Gamma^2_{oo'}(t) < 0$: repulsive correlation

doublon-holon

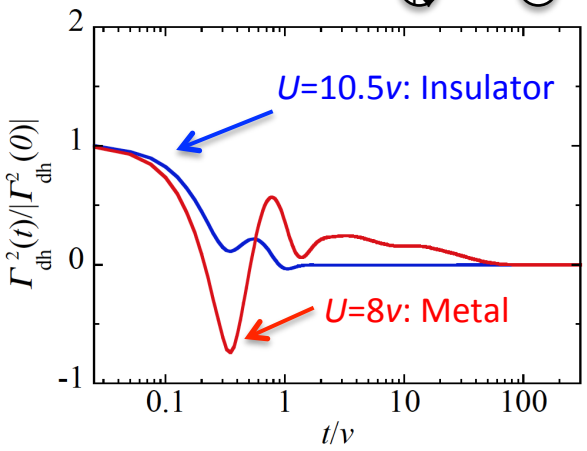

doublon-doublon

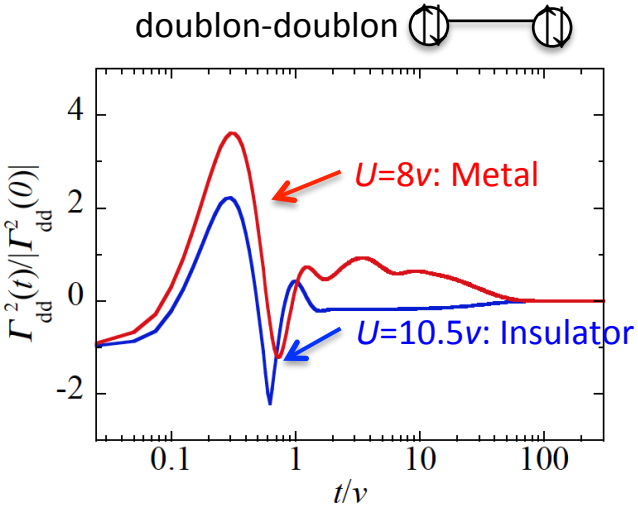

Holon-holon